

# Isomerism of Cp-Containing Transition Metal Allyl Complexes

Siwei Bi, Alireza Ariaafard, Guochen Jia,\* and Zhenyang Lin\*

Department of Chemistry and Open Laboratory of Chirotechnology of the Institute of Molecular Technology for Drug Discovery and Synthesis, The Hong Kong University of Science and Technology, Clear Water Bay, Kowloon, Hong Kong

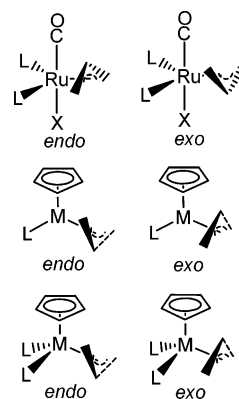
Received September 24, 2004

The isomerism of Cp-containing transition metal  $\eta^3$ -allyl complexes has been investigated with the aid of density functional theory calculations. The effect of ligands and numbers of metal d electrons on the isomerism has been examined and discussed in detail. Our studies show that  $d^6$ -CpML( $\eta^3$ -allyl) (L = CO, PR<sub>3</sub>, N≡CR, alkyl, hydride, halides) complexes preferentially adopt *exo* structural isomers in which the central allylic hydrogen (or substituent) of the  $\eta^3$ -allyl ligand points toward the Cp ring. However, when L =  $\eta^2$ -olefin, an *endo* form is preferred. For  $d^4$ -CpML<sub>2</sub>( $\eta^3$ -allyl) (L ≠ CO) complexes, *endo* isomers are preferred. When L = CO, *endo* and *exo* isomers have comparable stability. Orbital interaction models have been proposed to explain the different isomerism behaviors of the complexes.

## Introduction

Transition metal allyl complexes display rich chemistry and are of considerable importance in homogeneous catalysis, where they often represent key intermediates.<sup>1</sup> This article concerns the isomerism of  $\eta^3$ -allyl complexes.<sup>2</sup> For a given  $\eta^3$ -allyl complex with an unsymmetrical ligand environment, there are two possible structural arrangements for the  $\eta^3$ -allyl ligand, i.e., the *endo* and *exo* arrangements, depending on the relative orientations of the central carbon of the  $\eta^3$ -allyl ligand with respect to other ligands in the complex (Chart 1). In many Cp-free ruthenium carbonyl complexes Ru( $\eta^3$ -allyl)Cl(CO)L<sub>2</sub>, the *endo* structural form is found to be more stable than the *exo* structural form.<sup>3</sup> The isomerism of Ru( $\eta^3$ -allyl)Cl(CO)(PPh<sub>3</sub>)<sub>2</sub> was studied by us both experimentally and computationally in a recent paper.<sup>4</sup> It was found that the *endo* structural form is intrinsically more stable than the *exo*

Chart 1



form because the *endo* structural arrangement of the  $\eta^3$ -allyl ligand provides an optimal situation to maximize the Ru(d)-to-CO( $\pi^*$ ) back-bonding interaction.<sup>4</sup>

Continuing the interest in the isomerism of transition metal allyl complexes, we report our studies on the isomerism of Cp-containing  $\eta^3$ -allyl complexes in this paper. Transition metal Cp-containing allyl complexes display very interesting and rich *endo*–*exo* isomerism. Different from the Cp-free  $d^6$  complexes M( $\eta^3$ -allyl)Cl(CO)(PR<sub>3</sub>)<sub>2</sub> (M = Ru, Os), many  $d^6$ -CpML( $\eta^3$ -allyl) (M = Ru, Os; L = CO, PR<sub>3</sub>) complexes give more stable *exo* isomers in which the central allylic hydrogen (or substituent) of the  $\eta^3$ -allyl ligand points toward the Cp ring. Examples include CpRu(CO)( $\eta^3$ -C<sub>3</sub>H<sub>5</sub>),<sup>5</sup> ( $\eta^5$ -C<sub>9</sub>H<sub>7</sub>)M(CO)( $\eta^3$ -C<sub>3</sub>H<sub>5</sub>) (M = Fe, Ru),<sup>6</sup> CpFe(CO)( $\eta^3$ -C<sub>3</sub>H<sub>5</sub>),<sup>7</sup> Cp\*IrCl( $\eta^3$ -C<sub>3</sub>H<sub>5</sub>),<sup>8</sup> [Cp\*Ir(PMe<sub>3</sub>)( $\eta^3$ -C<sub>3</sub>H<sub>5</sub>)]<sup>+</sup>,<sup>9</sup> [Cp\*Ir(MeCN)( $\eta^3$ -CHPhCHCH<sub>2</sub>)]<sup>+</sup>, and [Cp\*Ir(MeCN)( $\eta^3$ -CH<sub>2</sub>CPhCH<sub>2</sub>)]<sup>+</sup>.<sup>10</sup> More interestingly, when L =  $\eta^2$ -olefin, the *endo* isomer is generally more stable. For example, both Cp\*Ru( $\eta^2$ -CH<sub>2</sub>=CH<sub>2</sub>)( $\eta^3$ -CH<sub>2</sub>CHCHMe)

\* To whom correspondence should be addressed. E-mail: chjiag@ust.hk; chzlin@ust.hk.

(1) (a) Consiglio, G.; Waymouth, R. M. *Chem. Rev.* **1989**, *89*, 257. (b) Tsuji, J. *Pure Appl. Chem.* **1989**, *61*, 1673. (c) Trost, B. M.; van Vranken, D. L. *Chem. Rev.* **1996**, *96*, 395. (d) Williams, J. M. J. *Adv. Asym. Synth.* **1996**, 299. (e) Helmchen, G.; Pfalz, A. *Acc. Chem. Res.* **2000**, *33*, 336. (f) Helmchen, G. *J. Organomet. Chem.* **1999**, *576*, 203. (g) Braunstein, P.; Zhang J.; Welter R. *Dalton Trans.* **2003**, 507.

(2) (a) John, K. D.; Salazar, K. V.; Scott, B. L.; Baker, R. T.; Sattelberger, A. P. *Chem. Commun.* **2000**, 581. (b) Chin, C. S.; Shin, S. Y.; Lee, C. *J. Chem. Soc., Dalton Trans.* **1992**, 1323. (c) Older, C. M.; Stryker, J. M. *Organometallics* **2000**, *19*, 2661. (d) Schwiebert, K. E.; Stryker, J. M. *Organometallics* **1993**, *12*, 600. (e) Wakefield, J. B.; Stryker, J. M. *J. Am. Chem. Soc.* **1991**, *113*, 7057. (f) Tjaden, E. B.; Stryker, J. M. *J. Am. Chem. Soc.* **1990**, *112*, 6420.

(3) (a) Wu, Y. M.; Wrighton, M. S. *Organometallics* **1988**, *7*, 1839. (b) Sakaki, S.; Ohki, T.; Takayama, T.; Sugimoto, M.; Kondo, T.; Mitsudo, T. *Organometallics* **2001**, *20*, 3145. (c) Sasabe, H.; Nakanishi, S.; Takata, T. *Inorg. Chem. Commun.* **2002**, *5*, 177. (d) Hiraki, K.; Matsunaga, T.; Kawano, H. *Organometallics* **1994**, *13*, 1878. (e) Hill, A. F.; Ho, C. T.; Wilton-Ely, D. E. T. *Chem. Commun.* **1997**, 2207. (f) Hiraki, K.; Ochi, N.; Sasada, Y.; Hayashida, H.; Fuchita, Y.; Yamanaka, S. *J. Chem. Soc., Dalton Trans.* **1985**, 873. (g) Barnard, C. F. J.; Daniels, B. J. A.; Holland, P. R.; Mawby, R. J. *J. Chem. Soc., Dalton Trans.* **1980**, 2418. (h) Cadierno, V.; Crochet, P.; Diez, J.; Garcia-Garrido, S. E.; Gimeno, J. *Organometallics* **2003**, *22*, 5226.

(4) Xue, P.; Bi, S.; Sung, H. H. Y.; Williams, I. D.; Lin, Z.; Jia, G. *Organometallics* **2004**, *23*, 4735.

and Cp\*Ru( $\eta^2$ -CH<sub>2</sub>CHMe)( $\eta^3$ -C<sub>3</sub>H<sub>5</sub>) have a more stable *endo* isomer.<sup>11</sup> For [Cp\*Ir( $\eta^2$ -C<sub>2</sub>H<sub>4</sub>)( $\eta^3$ -C<sub>3</sub>H<sub>5</sub>)]<sup>+</sup>, the *endo* isomer is also more stable than the *exo* isomer.<sup>12</sup> In d<sup>4</sup> CpML<sub>2</sub>( $\eta^3$ -allyl) complexes, the isomerism is more complicated. In general, the *endo* structural form is preferred. Complexes of this type include Cp\*OsX<sub>2</sub>( $\eta^3$ -CH<sub>2</sub>CMeCH<sub>2</sub>) (X = Br, Me, H),<sup>13</sup> CpRuX<sub>2</sub>( $\eta^3$ -C<sub>3</sub>H<sub>5</sub>) (X = Cl, Br),<sup>14</sup> CpRuCl<sub>2</sub>( $\eta^3$ -C<sub>4</sub>H<sub>4</sub>Ome),<sup>15</sup> Cp\*Ru-(CH<sub>2</sub>Cl)Cl( $\eta^3$ -C<sub>3</sub>H<sub>5</sub>),<sup>16</sup> CpRu(R)Br( $\eta^3$ -C<sub>3</sub>H<sub>5</sub>) (R = Me, CH<sub>2</sub>SiMe<sub>3</sub>),<sup>17</sup> and [Cp\*Ru(amidinate)( $\eta^3$ -C<sub>3</sub>H<sub>5</sub>)]<sup>+</sup>.<sup>18</sup> When L = CO, both the *endo* and *exo* structural forms have comparable stability.<sup>19–22</sup> For example, for Cp'Mo(CO)<sub>2</sub>( $\eta^3$ -C<sub>3</sub>H<sub>5</sub>) (Cp' = C<sub>5</sub>H<sub>4</sub>-C(O)-Phe-OMe) the *endo:exo* ratio is found to be 1:4,<sup>19</sup> while for CpMo(CO)<sub>2</sub>( $\eta^3$ -CH<sub>2</sub>CRCH<sub>2</sub>) (R = C(O)Me) the ratio was found to be 9:1.<sup>20</sup> For CpMo(CO)<sub>2</sub>( $\eta^3$ -CH<sub>2</sub>CRCH<sub>2</sub>) (R = H, Me), the *endo–exo* relative stability depends on whether R is H or Me.<sup>21</sup> Although there are a few theoretical studies of allyl complexes in the literature,<sup>3b,23</sup> studies on how the metal d electron counts and the types of ligands would affect the isomerism are still lacking.

### Computational Details

Geometry optimizations for all compounds without symmetry constraints were performed using density functional theory calculations at the Becke3LYP (B3LYP) level.<sup>24</sup> Frequency calculations at the same level of theory have also been performed to identify all stationary points as minima (zero imaginary frequency). The effective core potentials (ECPs) of Hay and Wadt with a double- $\zeta$  valence basis set (LanL2DZ)<sup>25</sup>

were used to describe Ru, Os, Ir, Cl, Br, and P. The 6-31G basis set was used for H, C, and O. Polarization functions were also added for C( $\zeta_d = 0.600$ ), O( $\zeta_d = 1.154$ ), Cl( $\zeta_d = 0.514$ ), Br( $\zeta_d = 0.389$ ), and P( $\zeta_d = 0.340$ ).<sup>26</sup> All calculations were performed with the use of the Gaussian 03 software package<sup>27</sup> on PC Pentium IV computers.

### Results and Discussion

**d<sup>6</sup>-CpML( $\eta^3$ -allyl) Complexes.** As mentioned in the Introduction, d<sup>6</sup> Cp-containing allyl complexes were found to preferentially adopt *exo* isomeric structures. The results of our density functional theory calculations on both the *exo* and *endo* structural isomers of CpRuL-( $\eta^3$ -CH<sub>2</sub>CHCH<sub>2</sub>) (L = CO, PH<sub>3</sub>), CpIrX( $\eta^3$ -CH<sub>2</sub>CHCH<sub>2</sub>) (X = Cl, H), and [CpIr(NCMe)( $\eta^3$ -CH<sub>2</sub>CHCH<sub>2</sub>)]<sup>+</sup> are consistent with the general observation that the *exo* isomers are found to be more stable. Figure 1 shows the results of relative energies together with selected structural parameters. From the structural parameters shown in Figure 1, we see that the metal– $\eta^3$ -allyl M–C bond distances for the *exo* isomers are in general shorter than those in the corresponding *endo* isomers, indicating that the higher stability of the *exo* isomers in comparison to their *endo* isomers is a result of stronger metal– $\eta^3$ -allyl interactions in the *exo* isomers.

To better understand the metal– $\eta^3$ -allyl interactions in these complexes, it is necessary to discuss the fragment orbitals of CpM. Figure 2 shows schematically the frontier orbitals for a d<sup>6</sup>-CpM metal fragment, the  $\pi$  orbitals of an  $\eta^3$ -allyl anionic ligand, and three types of relevant orbital interactions between CpM and  $\eta^3$ -allyl. The frontier orbitals of d<sup>6</sup>-CpM consist of three occupied metal d orbitals (d<sub>z<sup>2</sup></sub>, d<sub>xy</sub>, d<sub>x<sup>2</sup>-y<sup>2</sup></sub>), which are available for metal(d)-to-ligand( $\pi^*$ ) back-bonding interactions, and three unoccupied orbitals (2a<sub>1</sub>+e<sub>1</sub>), which can interact with orbitals accommodating ligands'  $\sigma$  electron pairs. In consideration of the high lying  $\pi_2$  orbital of the  $\eta^3$ -allyl ligand, it is expected that repulsive interaction between metal d electrons and  $\pi_2$  electrons is important.

On the basis of the discussion above, the orbital interaction diagram between d<sup>6</sup>-CpM and (L +  $\eta^3$ -allyl), shown in Figure 3, can be constructed. The three unoccupied frontier orbitals of CpM mainly interact with the three occupied orbitals from L and the  $\eta^3$ -allyl ligand, giving three bonding and three antibonding molecular orbitals. Among the three occupied d orbitals, d<sub>x<sup>2</sup>-y<sup>2</sup></sub> and d<sub>z<sup>2</sup></sub> are stabilized through their interaction

(5) (a) King, R. B.; Ishaq, M. *Inorg. Chim. Acta* **1970**, *4*, 258. (b) Gibson, D. H.; Hsu, W.-L.; Johnson, B. V. *J. Organomet. Chem.* **1981**, *208*, 89. (c) Hsu, L.-Y.; Nordman, C. E.; Gibson, D. H.; Hsu, W.-L. *Organometallics* **1989**, *8*, 241.

(6) Faller, J. W.; Johnson, B. V.; Dryja, T. P. *J. Organomet. Chem.* **1974**, *65*, 395.

(7) Fish, R. W.; Giering, W. P.; Marten, D.; Rosenblum, M. *J. Organomet. Chem.* **1976**, *105*, 101.

(8) Maghee, W. D.; Bergman, R. G. *J. Am. Chem. Soc.* **1988**, *110*, 4246.

(9) Burger, P.; Bergman, R. G. *J. Am. Chem. Soc.* **1993**, *115*, 10462.

(10) Jeong, H.; Joo, K.-S.; Chin, C. S. *Bull. Korean Chem. Soc.* **1997**, *18*, 402.

(11) Koelle, U.; Kang, B. S.; Spaniol, T. P.; Englert, U. *Organometallics* **1992**, *11*, 249.

(12) Wakefield, J. B.; Stryker, J. M. *Organometallics* **1990**, *9*, 2428.

(13) Mui, H. D.; Brumaghim, J. L.; Gross, C. L.; Girolami, G. S. *Organometallics* **1999**, *18*, 8, 3264.

(14) Nagashima, H.; Mukai, K.; Shiota, Y.; Yamaguchi, K.; Ara, K. I.; Fukahori, T.; Suzuki, H.; Akita, M.; Moro-oka, Y.; Itoh, K. *Organometallics* **1990**, *9*, 799.

(15) Albers, M. O.; Liles, D. C.; Robinson, D. J.; Shaver, A.; Singleton, E. *Organometallics* **1987**, *6*, 2347.

(16) Hubbard, J. L.; Zoch, C. R. *J. Organomet. Chem.* **1995**, *487*, 65.

(17) Itoh, K.; Fukahori, T. *J. Organomet. Chem.* **1988**, *349*, 227.

(18) Kondo, H.; Yamaguchi, Y.; Nagashima, H. *Chem. Commun.* **2000**, 1075.

(19) Dave, D. V. S.; Weyhermüller, T.; Metzler-Nolte, N. *Organometallics* **2000**, *19*, 3730.

(20) Liao, M.-F.; Lee, G.-H.; Peng, S.-M.; Liu, R.-S. *Organometallics* **1994**, *13*, 4973.

(21) Faller, J. W.; Incorvia, M. J. *Inorg. Chem.* **1968**, *7*, 840.

(22) Benyunes, S. A.; Binelli, A.; Green, M.; Grimshire, M. J. *J. Chem. Soc., Dalton Trans.* **1991**, 895.

(23) (a) Curtis, M. D.; Eisenstein, O. *Organometallics* **1984**, *3*, 887.

(b) Schiling, B. E. R.; Hoffmann, R.; Fallerlb, J. W. *J. Am. Chem. Soc.* **1979**, *101*, 592. (c) Webster, C. E.; Hall, M. B. *Organometallics* **2001**, *20*, 5606. (d) Ascenso, J. R.; de Azevedo, C. G.; Calhorda, M. J.; Carrondo, M.; Costa, P.; Dias, A. R.; Drew, M. G. B.; Felix, V.; Galvao, A. M.; Romao, C. C. *J. Organomet. Chem.* **2001**, *632*, 197. (e) Swang, O.; Blom, R. *J. Organomet. Chem.* **1998**, *561*, 29. (f) Suzuki, T.; Okada, G.; Hioki, Y.; Fujimoto, H. *Organometallics* **2003**, *22*, 3649.

(24) (a) Becke, A. D. *J. Chem. Phys.* **1993**, *98*, 5648. (b) Miehlich, B.; Savin, A.; Stoll, H.; Preuss, H. *Chem. Phys. Lett.* **1989**, *157*, 200. (c) Lee, C.; Yang, W.; Parr, G. *Phys. Rev.* **1988**, *B37*, 785.

(25) (a) Hay, P. J.; Wadt W. R. *J. Chem. Phys.* **1985**, *82*, 270. (b) Wadt, W. R.; Hay, P. J. *J. Chem. Phys.* **1985**, *82*, 284. (c) Hay, P. J.; Wadt, W. R. *J. Chem. Phys.* **1985**, *82*, 299.

(26) Hariharan, P. C.; Pople, J. A. *Theor. Chim. Acta* **1973**, *28*, 213.

(27) Frisch, M. J.; Trucks, G. W.; Schlegel, H. B.; Scuseria, G. E.; Robb, M. A.; Cheeseman, J. R.; Montgomery, J. A.; Vreven, J. T.; Kudin, K. N.; Burant, J. C.; Millam, J. M.; Iyengar, S. S.; Tomasi, J.; Barone, V.; Mennucci, B.; Cossi, M.; Scalmani, G.; Rega, N.; Petersson, G. A.; Nakatsuji, H.; Hada, M.; Ehara, M.; Toyota, K.; Fukuda, R.; Hasegawa, J.; Ishida, M.; Nakajima, T.; Honda, Y.; Kitao, O.; Nakai, H.; Klene, M.; Li, X.; Knox, J. E.; Hratchian, H. P.; Cross, J. B.; Adamo, C.; Jaramillo, J.; Gomperts, R.; Stratmann, R. E.; Yazyev, O.; Austin, A. J.; Cammi, R.; Pomelli, C.; Ochterski, J. W.; Ayala, P. Y.; Morokuma, K.; Voth, G. A.; Salvador, P.; Dannenberg, J. J.; Zakrzewski, V. G.; Dapprich, S.; Daniels, A. D.; Strain, M. C.; Farkas, O.; Malick, D. K.; Rabuck, A. D.; Raghavachari, K.; Foresman, J. B.; Ortiz, J. V.; Cui, Q.; Baboul, A. G.; Clifford, S.; Cioslowski, J.; Stefanov, B. B.; Liu, G.; Liashenko, A.; Piskorz, P.; Komaromi, I.; Martin, R. L.; Fox, D. J.; Keith, T.; Al-Laham, M. A.; Peng, C. Y.; Nanayakkara, A.; Challacombe, M.; Gill, P. M. W.; Johnson, B.; Chen, W.; Wong, M. W.; Gonzalez, C.; Pople, J. A. *Gaussian 03*, revision B05; Gaussian, Inc.: Pittsburgh, PA, 2003.

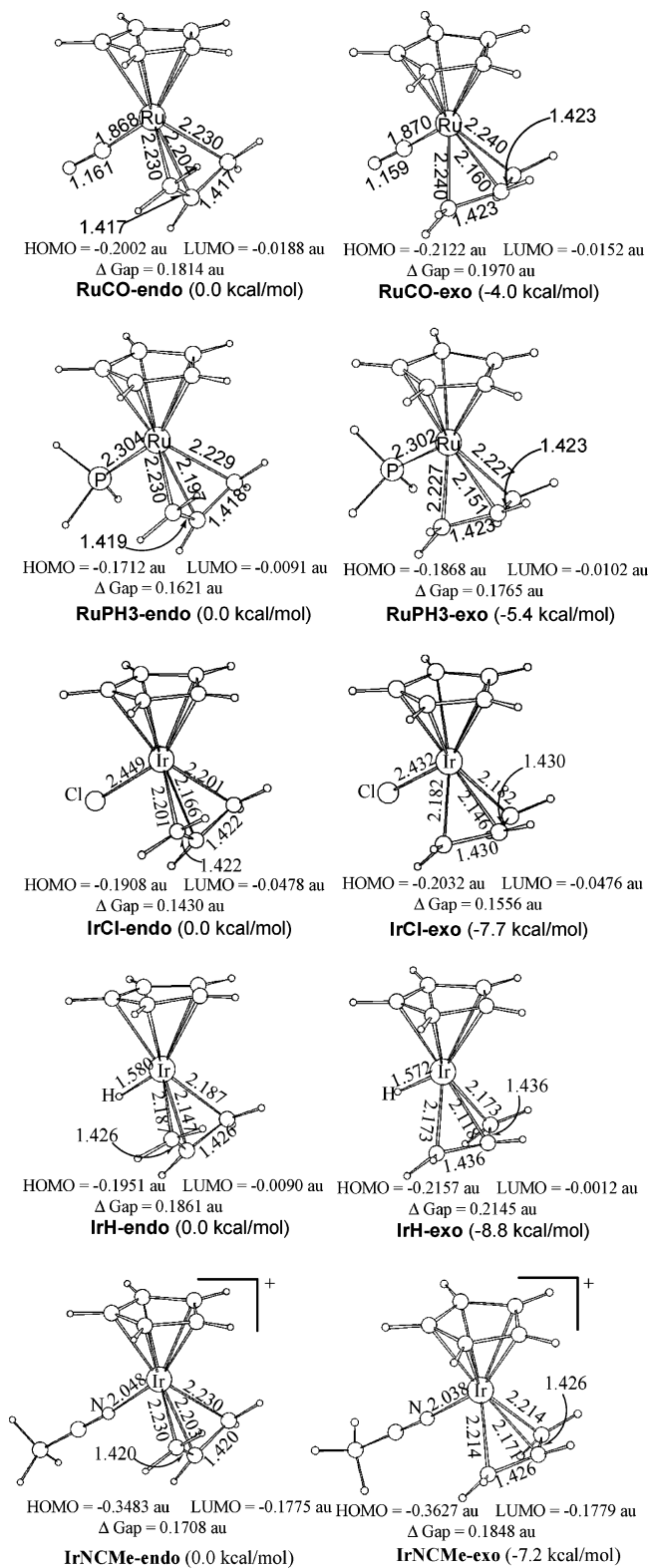


**Figure 1.** Optimized structures of species having a general formula of  $d^6\text{-CpML}(\eta^3\text{-allyl})$ .

with  $\pi_3$ , while the  $d_{xy}$  orbital is destabilized due to the four-electron repulsive interaction with the occupied  $\pi_2$  orbital. For simplicity, the  $\pi$  orbitals of L are omitted from Figure 3. The omission should not affect application of the diagram to the systems studied here in view of the fact that the *exo* isomers are more stable than the *endo* isomers regardless of having  $\pi$ -donating L,  $\pi$ -neutral L, or  $\pi$ -accepting L (see Figure 1).

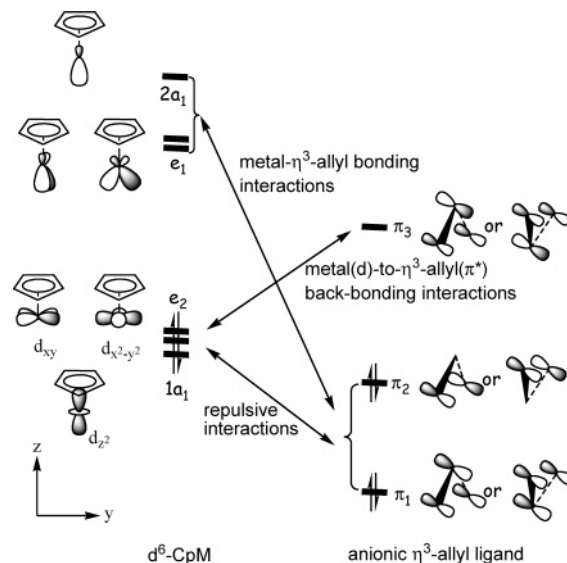


**Figure 2.** Schematic illustration of the three types of orbital interactions between a CpM metal fragment and an  $\eta^3$ -allyl ligand.

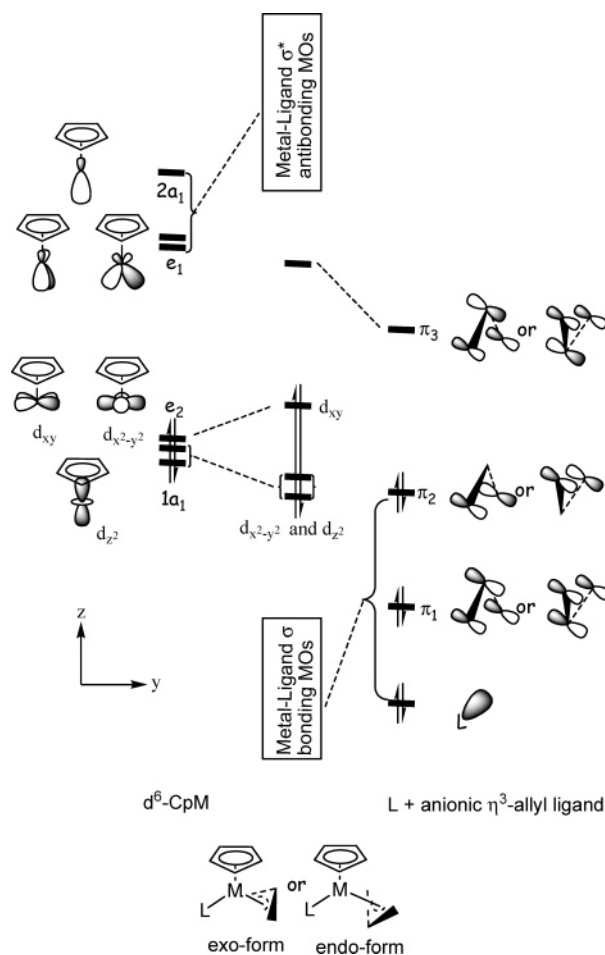
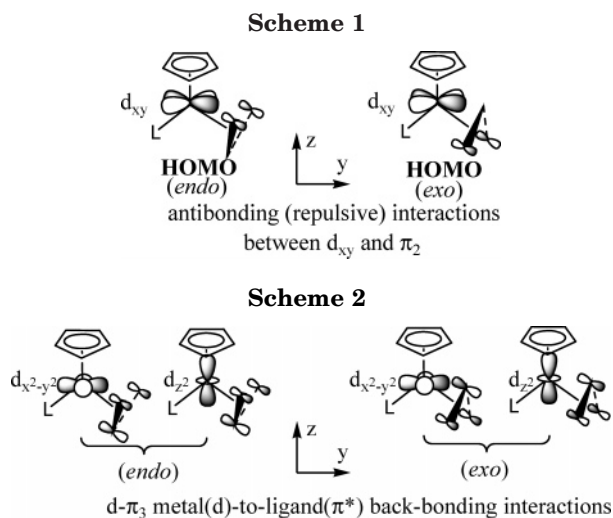


**Figure 3.** Orbital interaction diagram for a  $d^6\text{-CpML}(\eta^3\text{-allyl})$  complex.

The question now is what factors govern the isomeric preference. The molecular orbitals derived from the orbital interactions between the three unoccupied frontier orbitals ( $2a_1 + e_1$ ) of CpM and the orbitals from the allyl ligand and L are not lying in the frontier region (Figure 3). Therefore, we anticipate that these molecular orbitals play less important roles in determining the



*exo*-*endo* relative stability. The  $d_{xy}$ - $\pi_2$  repulsive interaction and the  $d$ - $\pi_3$  back-bonding interactions, which give rise to the frontier molecular orbitals, are expected to be important to the stability difference between the *exo* and *endo* isomers. Scheme 1 illustrates the  $d_{xy}$ - $\pi_2$  repulsive interaction for both *endo* and *exo* structural arrangements. Significant difference in the repulsive interaction can be seen between the two structural arrangements. The  $d_{xy}$ - $\pi_2$  repulsive interaction in the *endo* isomers is more significant because of the better orbital overlap (Scheme 1). The *exo* isomers are expected to experience weaker  $d_{xy}$ - $\pi_2$  repulsive interaction. Scheme 2 illustrates the  $d$ - $\pi_3$  back-bonding interactions for both the *endo* and *exo* structural arrangements. We can see that the *endo* arrangement has a better orbital overlap between  $d_{xy}$  and  $\pi_3$ , but a poorer one between  $d_{x^2-y^2}$  and  $\pi_3$ . A reverse situation is found for the *exo* arrangement; that is, the  $d_{x^2-y^2}$  orbital overlaps with the  $\pi_3$  orbital better. In comparison to  $d_{xy}$ ,  $d_{x^2-y^2}$  is higher in energy and better for back-bonding interaction due to the  $\sigma^*$ -antibonding character with L. Therefore, the back-bonding interactions also favor the *exo* structural arrangement.

In summary, the smaller  $d_{xy}$ - $\pi_2$  repulsive interaction and greater  $d$ - $\pi_3$  back-bonding interactions in the *exo* structural arrangement are responsible for the observed stronger metal- $\eta^3$ -allyl bonding interactions. The arguments here are supported by the molecular orbital calculations. The  $d_{xy}$  orbital, which is weakly antibonding with  $\pi_2$ , is found to be the highest occupied molecular orbital (HOMO) for all the structures shown in Figure 1, indicating the importance of the  $d_{xy}$ - $\pi_2$  repulsive interaction. Figure 4 gives the plots of the HOMOs for both the *endo* and *exo* isomers of CpIrH-( $\eta^3$ -allyl), showing the  $d_{xy}$ - $\pi_2$  antibonding interaction. The results of calculations also show that all the *exo* isomers, which have smaller  $d_{xy}$ - $\pi_2$  repulsive interaction, have more stable HOMOs and larger HOMO-LUMO gaps than their *endo* counterparts (see Figure 1). The  $d_{x^2-y^2}$  orbital is found to be the second highest occupied molecular orbital. Again, all the calculated *exo* isomers, which have better  $d_{x^2-y^2}$ - $\pi_3$  back-bonding interaction, have more stable second-HOMOs than their *endo* counterparts.

The qualitative arguments above also find support from our charge decomposition analysis (CDA) calcula-

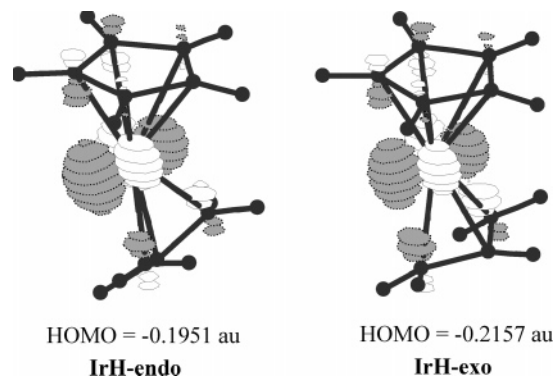
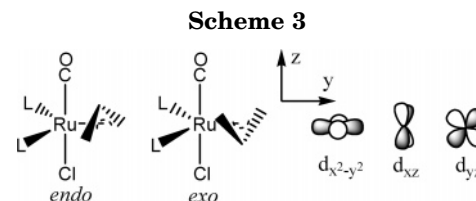


**Figure 4.** Spatial plots of the HOMOs for both the *endo* and *exo* isomers of CpIrH( $\eta^3$ -allyl).



tions.<sup>28</sup> The more stable *exo* isomers have more significant electron donation from the  $\eta^3$ -allyl anionic ligand to the metal fragments as well as more significant back-donation from the metal fragments to the  $\pi_3$  orbital of the  $\eta^3$ -allyl ligand than their less stable *endo* counterparts. For example, electron donation of 0.895e and back-donation of 0.214e were calculated for **RuCO-*exo***. Smaller electron donation of 0.857e and smaller back-donation of 0.171e were calculated for **RuCO-*endo***. For the iridium chloride complex, electron donation of 0.898e and back-donation of 0.249e were calculated for **IrCl-*exo***. Smaller electron donation of 0.823e and smaller back-donation of 0.215e were calculated for **IrCl-*endo***.

For the two ruthenium complexes, the *endo*-*exo* energy differences do not differ much (Figure 1). Among the three iridium complexes, the *endo*-*exo* energy differences are also close to each other. These results suggest that the *endo*-*exo* energy differences in these d<sup>6</sup>-CpML( $\eta^3$ -allyl) complexes are mainly related to the differences in the metal- $\eta^3$ -allyl interactions between the two isomeric structural forms. The three iridium complexes have greater *endo*-*exo* energy differences than the two ruthenium complexes, a result of stronger Ir- $\eta^3$ -allyl interactions than Ru- $\eta^3$ -allyl interactions, as evidenced by the metal- $\eta^3$ -allyl bond distances.

We now come to understand the reason why the isomerism in Ru( $\eta^3$ -allyl)Cl(CO)(PR<sub>3</sub>)<sub>2</sub>, in which the *endo* isomer was found to be intrinsically more stable than the corresponding *exo* isomer, is quite different from what we see in the CpRuL( $\eta^3$ -allyl) (L = CO, PR<sub>3</sub>) complexes, although CpRuL is isolobal with RuCl(CO)-(PR<sub>3</sub>)<sub>2</sub>. In Ru( $\eta^3$ -allyl)Cl(CO)(PR<sub>3</sub>)<sub>2</sub>, there are no  $d$ - $\pi_2$  repulsive interactions because the three d orbitals that accommodate the metal d electrons are very different from those in the Cp complexes. Scheme 3 shows the three occupied metal d orbitals that are available for metal(d)-to-ligand( $\pi^*$ ) back-bonding interactions. The  $d_{x^2-y^2}$  orbital interacts with the  $\pi_3$  orbital from the allyl ligand while the  $d_{xz}$  and  $d_{yz}$  orbitals mainly interact with

(28) Dapprich, S.; Frenking, G. CDA 2.1; 1994. The program is available via: ftp.chemie.uni-marburg.de/pub/cda.

the  $\pi^*$  orbitals of the carbonyl ligand. It is because there is no  $d-\pi_2$  repulsive interaction and  $d_{x^2-y^2}-\pi_3$  back-bonding interaction does not differ much between the *endo* and *exo* structural arrangements in the Cp-free complexes that their isomerism is mainly governed by the metal(d)-to-CO( $\pi^*$ ) back-bonding interaction. The *endo* structural arrangement provides an optimal situation to maximize the Ru(d)-to-CO( $\pi^*$ ) back-bonding interaction because the two strong Ru-C(terminal) bonds form larger angles with the CO ligand.<sup>4</sup>

**$d^6$ -CpM(olefin)( $\eta^3$ -allyl) Complexes.** Compared to the  $d^6$ -CpML( $\eta^3$ -allyl) complexes discussed above,  $d^6$ -CpM(olefin)( $\eta^3$ -allyl) complexes display different isomerism in which the *endo* isomeric form is found to be slightly more stable than the *exo* isomeric form. Figure 5 shows structures and relative energies of two calculated complexes. The results are consistent with the isomerism observed experimentally and summarized in the Introduction. The osmium complex has a greater *endo-exo* energy difference than the ruthenium complex, reflecting stronger osmium-ligand interactions. Olefin ligands differ from the ligands studied in the preceding section in that an  $\eta^2$ -olefin is a very strong single-face  $\pi$ -accepting ligand. Examining the structural arrangement of the olefin ligand in the structures calculated (Figure 5), we can see that the  $d_{xy}$  orbital is used for the metal(d)-to-olefin( $\pi^*$ ) back-bonding interaction. Because of the metal(d)-to-olefin( $\pi^*$ ) back-bonding interaction, the  $d_{xy}-\pi_2$  repulsive interaction becomes not a problem for the *endo* structural form in the  $d^6$ -CpM(olefin)( $\eta^3$ -allyl) complexes. A push-pull of allyl( $\pi_2$ )-to-metal( $d_{xy}$ )-to-olefin( $\pi^*$ ) bonding scenario is actually achieved in these olefin complexes. The results of our calculations indicate that the push-pull bonding interaction significantly enhances both the metal- $\eta^2$ -olefin and metal- $\eta^3$ -allyl bonding interactions, evidenced by their shorter bond distances in the more stable *endo* isomers (Figure 5). Clearly, the push-pull interaction is so dominant in the olefin complexes that the difference in the  $d-\pi_3$  back-bonding interactions between the two structural forms becomes unimportant to their stability difference.

In addition to the push-pull factor, there is another very important factor that also contributes to the switching of the isomerism in these olefin complexes. The greater ligand-ligand repulsion in the *exo* arrangement due to the more sterically demanding olefin ligand in comparison to CO and phosphines results in asymmetric coordination of both  $\eta^3$ -allyl and  $\eta^2$ -olefin in the *exo* isomeric structural form (Figure 5), giving the instability of the *exo* isomers and relatively stabilizing the *endo* isomers. To further support the steric arguments here, we carried out calculations of several osmium complexes in which the olefin and  $\eta^3$ -allyl ligands have methyl substituent(s) (Figure 5). We can see from Figure 5 that the *endo-exo* energy differences for the osmium complexes increase with the number of methyl substituents, supporting the arguments that the ligand-ligand repulsive interaction is more significant in the *exo* isomers.

**$d^4$ -CpML<sub>2</sub>( $\eta^3$ -allyl) Complexes.** To study the isomerism of  $d^4$ -CpML<sub>2</sub>( $\eta^3$ -allyl) complexes, we calculated CpRuCl<sub>2</sub>( $\eta^3$ -allyl), CpMo(PH<sub>3</sub>)<sub>2</sub>( $\eta^3$ -allyl), and CpMo(CO)<sub>2</sub>( $\eta^3$ -allyl). The results, shown in Figure 6, are quite

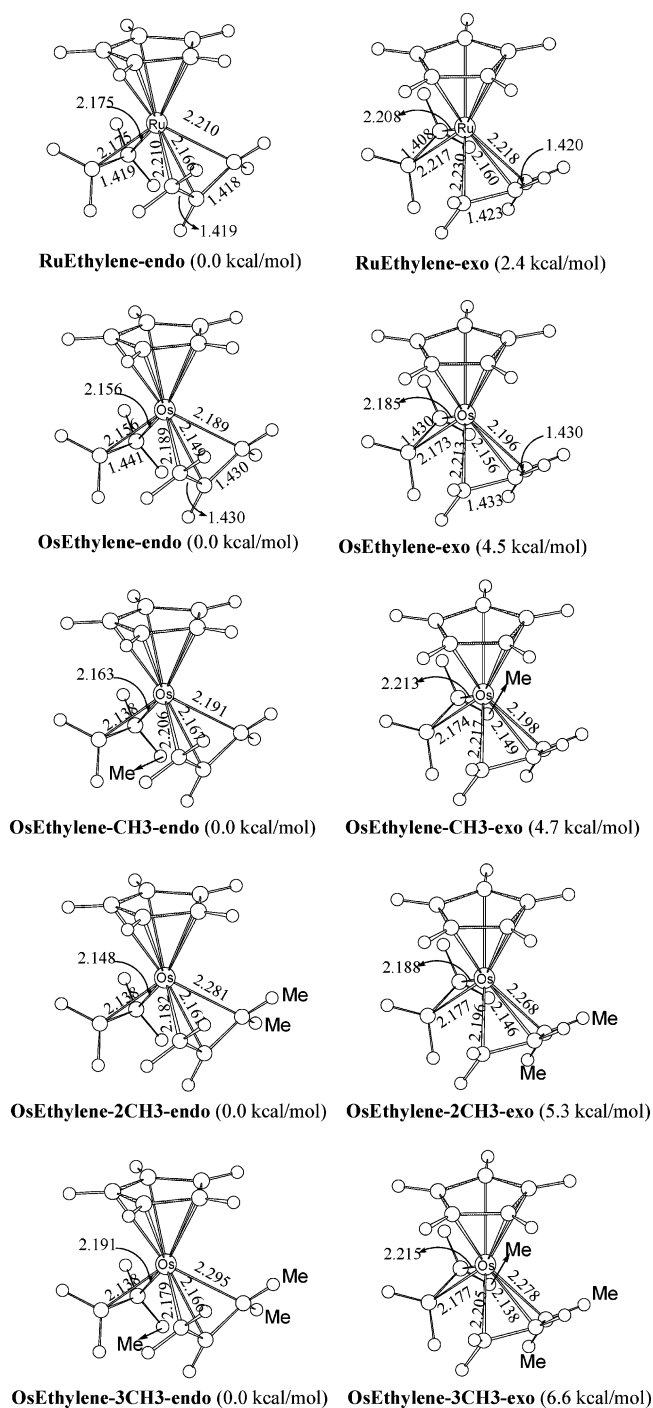


**Figure 5.** Optimized structures of representative  $d^6$ -CpM( $\eta^2$ -olefin)( $\eta^3$ -allyl).

interesting. In the former two complexes, the *endo* isomers are found to be more stable and the ruthenium chloride complex has a much greater *endo-exo* energy difference than the molybdenum phosphine complex. In the molybdenum carbonyl complex, the *exo* isomer is, however, slightly more stable than the *endo* isomer.

CpML<sub>2</sub>( $\eta^3$ -allyl) can be formally viewed as having a four-legged piano-stool structure when the  $\eta^3$ -allyl ligand is considered as forming two  $\sigma$  bonds with the metal center from its occupied  $\pi_1$  and  $\pi_2$  orbitals. In a  $d^4$  CpML<sub>2</sub>( $\eta^3$ -allyl) complex, the four metal d electrons occupy the  $d_{x^2-y^2}$  and  $d_{z^2}$  orbitals, which are available for back-bonding interactions. There are no d electrons

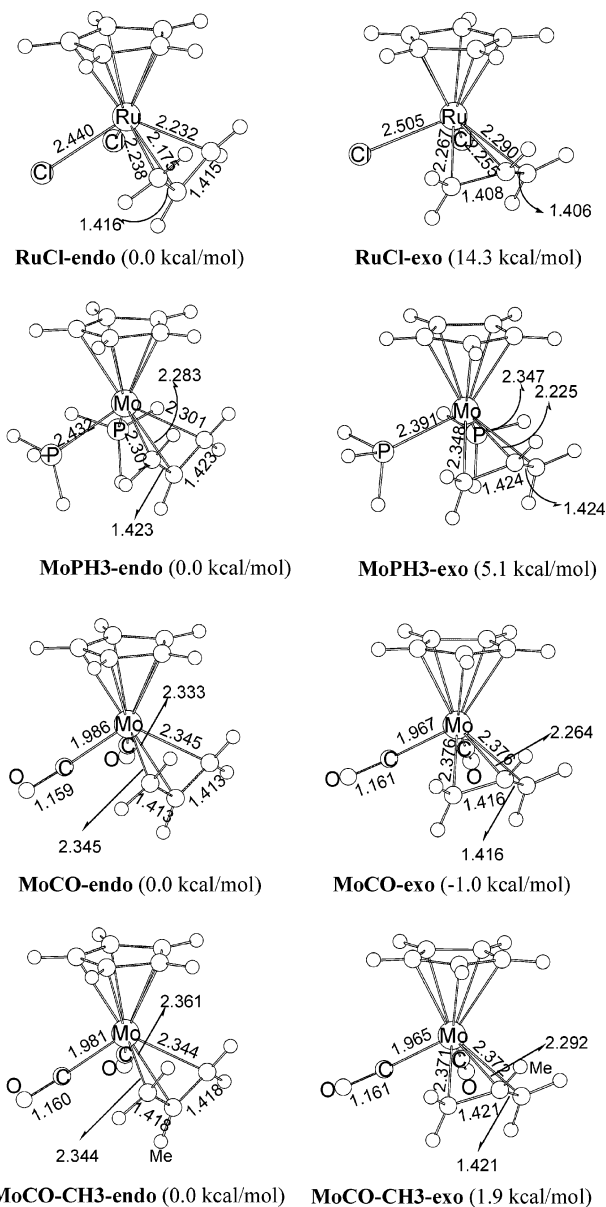
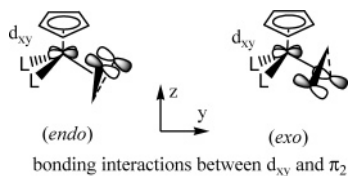


**Figure 6.** Optimized structures of species having a general formula of  $d^4\text{-CpML}_2(\eta^3\text{-allyl})$ .

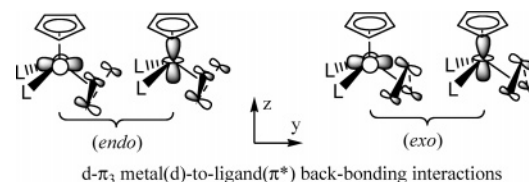
#### Scheme 4



in the  $d_{xy}$  orbital because  $d_{xy}$  is involved in the metal-ligand  $\sigma$ -bonding.

Because of no d electrons in the  $d_{xy}$  orbital, the  $d_{xy}-\pi_2$  interaction becomes stabilizing rather than destabilizing like in the case of  $d^6$   $\text{CpML}(\eta^3\text{-allyl})$  complexes. Since the  $d_{xy}-\pi_2$  interaction is stabilizing, the *endo* arrangement favors the interaction because of better orbital overlap (Scheme 4). In the  $d-\pi_3$  back-bonding interactions, both the  $d_{x^2-y^2}$  and  $d_{z^2}$  orbitals are involved. Again, there is a better orbital overlap between  $d_{z^2}$  and  $\pi_3$  but a poorer one between  $d_{x^2-y^2}$  and  $\pi_3$  for the *endo* arrangement, and vice versa for the *exo* arrangement (Scheme 5). We argue here that the *endo*

#### Scheme 5



arrangement also favors the  $d-\pi_3$  back-bonding interactions because  $d_{z^2}$  has a greater back-bonding capability than  $d_{x^2-y^2}$  due to its higher orbital energy, which has been well recognized in four-legged piano-stool complexes.<sup>29</sup> Unlike in  $\text{CpML}(\eta^3\text{-allyl})$ ,  $d_{x^2-y^2}$  in  $\text{CpML}_2(\eta^3\text{-allyl})$  does not have  $\sigma^*$ -antibonding character, with the two L ligands residing on the nodal planes. This is the reason  $d_{x^2-y^2}$  is lower in energy than  $d_{z^2}$  in a four-legged piano-stool complex but vice versa in a three-legged complex. Sterically, the *endo* arrangement is also favorable. In the *exo* arrangement, the C-C-C moiety eclipses the two M-L bonds, giving significant repulsive interactions. Summarizing all the arguments, the *endo* structural form in a  $d^4$   $\text{CpML}_2(\eta^3\text{-allyl})$  complex is intrinsically more stable both electronically and sterically.

The ruthenium chloride complex has a greater *endo-exo* energy difference than the molybdenum phosphine complex. Chloride ligands possess good  $\pi$ -donating properties, enhancing the  $d-\pi_3$  back-bonding interactions. Therefore, the difference derived from the back-bonding interactions between the two different structural isomers is expected to be significant.

The molybdenum carbonyl complex is interesting (Figure 6), as the *exo* isomer is more stable than the *endo* isomer, although we concluded that the *endo* structural form is intrinsically more stable than the *exo* form. To understand the unusual behavior of this complex, we again have to analyze the following two aspects: (1) the  $d_{xy}-\pi_2$  bonding interaction and (2)  $d-\pi_3$  back-bonding interactions, which are important in determining the *endo-exo* relative stability as mentioned above. (1) In terms of the  $d_{xy}-\pi_2$  bonding interaction, we still see that the *endo* isomer still favors this interaction, as the Mo-C(terminal) bonds of the Mo- $\eta^3$ -allyl moiety in the **MoCO-endo** isomer are shorter than those in the **MoCO-exo** isomer (Figure 6). However, because of the strong Mo-CO bonding interactions, the weakened Mo-C(terminal) bonds due to poorer  $d_{xy}-\pi_2$  interaction in the **MoCO-exo** isomer have been compensated by the strengthened Mo-CO bonds; that is, the **MoCO-exo** isomer has shorter Mo-CO bonds (Figure 6). The energy gained from the strengthened Mo-CO interactions seems to balance the energy lost from the weakened Mo-C(terminal) bonding interactions. (2) As mentioned above, the *endo* structural form favors the  $d-\pi_3$  back-bonding interactions because the  $d_{z^2}$  orbital has a better donating capability. Since CO is also a very strong  $\pi$ -accepting ligand, carbonyl  $\pi^*$  orbitals are expected to prefer to interact with the  $d_{z^2}$  orbital in the back-bonding interaction. Therefore, the *endo* structural form in the molybdenum carbonyl complex expects to experience a fierce competition for metal(d)-to-ligand( $\pi^*$ ) back-donation between the two

(29) (a) Cubacek, P.; Hoffmann, R.; Havlas, Z. *Organometallics* **1982**, *1*, 180. (b) Poli, R. *Organometallics* **1990**, *9*, 1892. (c) Lin, Z.; Hall, M. B. *Organometallics* **1993**, *12*, 19.

carbonyls and the  $\eta^3$ -allyl ligand. This is because of the competition that destabilizes the *endo* isomer, giving a more stable *exo* isomer in the carbonyl complex. The competition for back-bonding interactions indeed weakens significantly the Mo–C(central) bond of the Mo– $\eta^3$ -allyl moiety in the **MoCO-endo** isomer; that is, the Mo–C(central) bond in the **MoCO-endo** isomer is much longer than that in the **MoCO-exo** isomer (Figure 6).

On the basis of the arguments above, we can come to the following conclusion. It is the competition for back-bonding interactions that makes the **MoCO-endo** isomer less favorable. Here, one may ask whether there is similar competition in the  $d^6$  CpRu(CO)( $\eta^3$ -allyl) complex. The answer is that the competition is not significant because the metal center in these  $d^6$  complexes has three occupied d orbitals. The CO ligand mainly looks for  $d_{z^2}$  and  $d_{xy}$  for back-bonding interactions, while the  $\eta^3$ -allyl ligand can use  $d_{x^2-y^2}$  to avoid competition. In the  $d^4$  complexes, the competition becomes significant because there are less metal d electrons available for back-bonding interactions.

The small energy difference between the *endo* and *exo* isomers calculated for the CpMo(CO)<sub>2</sub>( $\eta^3$ -allyl) model complex (Figure 6) explains the experimental observation that both the *endo* and *exo* isomers of Cp'Mo(CO)<sub>2</sub>( $\eta^3$ -allyl) (Cp' = C<sub>5</sub>H<sub>4</sub>-C(O)-Phe-OMe)<sup>19</sup> are present in solution in a ratio of 1:4 on the basis of H<sup>1</sup> NMR spectroscopy. The small energy difference also allows us to understand an earlier experiment showing that a Me substituent at the central carbon of the  $\eta^3$ -allyl ligand in CpMo(CO)<sub>2</sub>( $\eta^3$ -allyl) switches the *exo-endo* relative stability.<sup>21</sup> Calculations of CpMo(CO)<sub>2</sub>( $\eta^3$ -H<sub>2</sub>-CCMeCH<sub>2</sub>) indeed show that the *endo* isomer becomes slightly more stable (Figure 6).

The recently characterized  $\{[\eta^5, \eta^1\text{-C}_5\text{H}_4(\text{CH}_2)_2\text{NMe}_2]\text{V}(\eta^3\text{-C}_3\text{H}_5)(\text{PMe}_3)\}^+$  complex<sup>30</sup> requires some comments here. Instead of having a  $d^4$  metal center, the complex has a  $d^2$  metal center. Similar to other carbonyl-free  $d^4$  complexes, this  $d^2$  complex also adopts an *endo* structure. Adoption of the *endo* structure suggests that the two d electrons occupy the  $d_{z^2}$  orbital, having better metal(d)-to- $\eta^3$ -allyl( $\pi^*$ ) back-bonding interaction. It should be noted that the arguments discussed above for CpMo(CO)<sub>2</sub>( $\eta^3$ -allyl) are also applicable to the analogous [CpMo(CO)(NO)( $\eta^3$ -allyl)]<sup>+</sup> complexes.<sup>31</sup>

### Conclusions

Transition metal  $\eta^3$ -allyl complexes display interesting isomerism. Cp-containing  $\eta^3$ -allyl complexes are

unique when compared to Cp-free complexes and show different isomeric preference from one type of complexes to another. In  $d^6$ -CpML( $\eta^3$ -allyl) complexes, the *exo* structural form is more stable than the *endo* one. The *exo* structural arrangement of the  $\eta^3$ -allyl ligand avoids repulsive interaction between one pair of d electrons and the  $\pi_2$  electrons from the  $\eta^3$ -allyl ligand and favors the metal(d)-to- $\eta^3$ -allyl( $\pi^*$ ) back-bonding interactions. When L = olefin, the *endo* structural form interestingly becomes more stable than the *exo* form. In the *endo* structural form, the  $\pi^*$  orbital of the very strong single-face  $\pi$ -accepting  $\eta^2$ -olefin ligand stabilizes significantly the pair of d electrons that are responsible for the repulsive interaction in the olefin-free  $d^6$ -CpML( $\eta^3$ -allyl) complexes. The d– $\pi_2$  repulsive interaction becomes no longer a problem for the  $d^6$ -CpM( $\eta^2$ -olefin)( $\eta^3$ -allyl) complexes. In addition, the more strictly demanding  $\eta^2$ -olefin in comparison to other ligands L, such as CO or phosphines, disfavors the *exo* structural form because of the more crowded ligand arrangement, giving a more stable *endo* structural form for  $d^6$ -CpM( $\eta^2$ -olefin)( $\eta^3$ -allyl) complexes. In  $d^4$ -CpML<sub>2</sub>( $\eta^3$ -allyl) complexes, the *endo* structural form is found to be intrinsically more stable. Because of two d electrons less than the  $d^6$  complexes, the d– $\pi_2$  interaction becomes stabilizing and favors the *endo* structural form. The *endo* arrangement of the  $\eta^3$ -allyl ligand also minimizes the ligand–ligand repulsion and has greater metal(d)-to- $\eta^3$ -allyl( $\pi^*$ ) back-bonding interactions due to the favorable orbital overlap between  $\pi^*$  of the  $\eta^3$ -allyl ligand and the better  $\pi$ -base metal  $d_{z^2}$  orbital observed in a four-legged piano-stool complex. When L = CO, both the *endo* and *exo* structural forms are found to have comparable stability. CO is a strong double-face  $\pi$ -accepting ligand that requires four metal d electrons for back-bonding interactions. The *endo* structural arrangement of the  $\eta^3$ -allyl ligand creates an unfavorable situation in that the  $\eta^3$ -allyl ligand competes against CO for back-bonding interactions, significantly weakening the metal–carbonyl bonding interactions, destabilizing the *endo* form, and making the *endo* form comparable in stability to the *exo* form.

**Acknowledgment.** The authors acknowledge financial support from the Hong Kong Research Grants Council (HKUST 6090/02P, HKUST 6023/04P, and DAG03/04.SC15) and the University Grants Committee of Hong Kong through the Area of Excellence Scheme (Aoe/P-10/01).

OM049256U

(30) Liu, G.; Beetstra, D. J.; Meetsma, A.; Hessen, B. *Organometallics* **2004**, *23*, 3914.

(31) Cosford, N. D. P.; Liebeskind, L. S. *Organometallics* **1994**, *13*, 1498.